Letter

Cynaropicrin Targets EGFR and MET Kinases and Promotes ROS Generation to Trigger Apoptosis and Ferroptosis in Non-small Cell Lung Cancer Cells

A-Young Nam[1,&], Na Yeong Lee[1,&], Goo Yoon[2], Jin Woo Park[1,2], Yung Hyun Choi[3], Joon-Seok Choi[4], Sang Hoon Joo[4,#], and Jung-Hyun Shim[1,2,5,#]

Non-small cell lung cancer (NSCLC), the most common type of lung cancer, is frequently linked to mutations, and there is a critical need to develop novel anticancer therapies that can circumvent resistance to existing targeted treatments. Co-targeting epidermal growth factor receptor (EGFR) and mesenchymal-epithelial transition factor (MET) may provide an effective approach to overcome genetic alterations in either pathway[1]. We aimed to explore an alternative approach for treating NSCLC cells that exhibit resistance to targeted therapy. HCC827GR cells, which are derived from HCC827 cells cultured in the presence of gefitinib (GEF)[2], serve as a cellular model for investigating GEF resistance in cancer. The resistance mechanisms of HCC827GR cells involve amplification of the gene encoding MET kinase and are linked to elevated reactive oxygen species (ROS) levels as well[3]. Cynaropicrin (Cyn) is a sesquiterpene lactone compound isolated from the artichoke[4], and we have recently documented its anticancer effects in colorectal cancer cells[5]. Evidence indicates that additional forms of programmed cell death may also contribute to the cytotoxicity induced by Cyn. In this study, we evaluated the anticancer potential of Cyn against HCC827 NSCLC cells both with and without GEF-resistance. Our findings suggest that Cyn is able to induce both apoptosis and ferroptosis in HCC827 cells.

To investigate the potential cytotoxicity of Cyn in NSCLC cells, HCC827 and HCC827GR cells were incubated with increasing doses of Cyn (0.2, 0.4, and 0.8 μg/mL) for 24 and 48 h. The MTT cell viability assay showed that Cyn diminished the viability and proliferation of NSCLC cells in a dose-dependent fashion. In contrast, Cyn did not elicit significant effects on the viability of HEKa cells (Figure 1A). The half inhibitory concentration (IC_{50}) values for Cyn after 48 h treatment in HCC827, HCC827GR, and HEKa cells were 1.67 μmol/L (0.58 μg/mL), 1.29 μmol/L (0.45 μg/mL), and 4.18 μmol/L (1.45 μg/mL), respectively. The selectivity indices of Cyn, non-cancer cells *vs.* cancer cells, were 2.5 for HCC827 and 3.3 for HCC827GR cells, demonstrating notable selectivity. The cancer-selective cytotoxicity of Cyn was shown in the soft-agar assay as well (Supplementary Figure S1). To examine whether Cyn-induced cytotoxicity was involved with the inhibition of the kinase activities of EGFR, MET, and AKT, we performed an in vitro kinase assay using recombinant kinases. Cyn exhibited potent inhibitory effects on EGFR and MET activity, whereas no inhibition was detected for AKT1 and AKT2 (Figure 1B). The IC_{50} values of Cyn for inhibition of EGFR and MET were 1.35 μmol/L (0.47 μg/mL) and 1.46 μmol/L (0.58 μg/mL), respectively. The in vitro ATP-competitive binding assay clearly demonstrated that the interaction between Cyn and EGFR or MET kinases could be displaced by ATP (Figure 1C). Moreover, Cyn treatment reduced the phosphorylation of EGFR, MET, and AKT kinases in HCC827 and HCC827GR cells (Figures 1D–1F, and Supplementary Figure 2). The inhibition of EGFR and MET kinases by Cyn is consistent with the molecular docking simulations performed with AutoDock Vina[6], which predicts that Cyn occupies the ATP binding sites of EGFR and MET kinases (Supplementary Figure S2B). Our findings suggest that Cyn treatment reduces the phosphorylation of EGFR and MET and subsequently influences the

doi: 10.3967/bes2026.104

1. Department of Biomedicine, Health & Life Convergence Sciences, BK21 Four, College of Pharmacy, Mokpo National University, Muan 58554, Republic of Korea; 2. Department of Pharmacy, College of Pharmacy, Mokpo National University, Muan 58554, Republic of Korea; 3. Department of Biochemistry, College of Korean Medicine, Dong-Eui University, Busan 47227, Republic of Korea; 4. College of Pharmacy, Daegu Catholic University, Gyeongsan 38430, Republic of Korea; 5. The China-US (Henan) Hormel Cancer Institute, Zhengzhou 450008, Henan, China

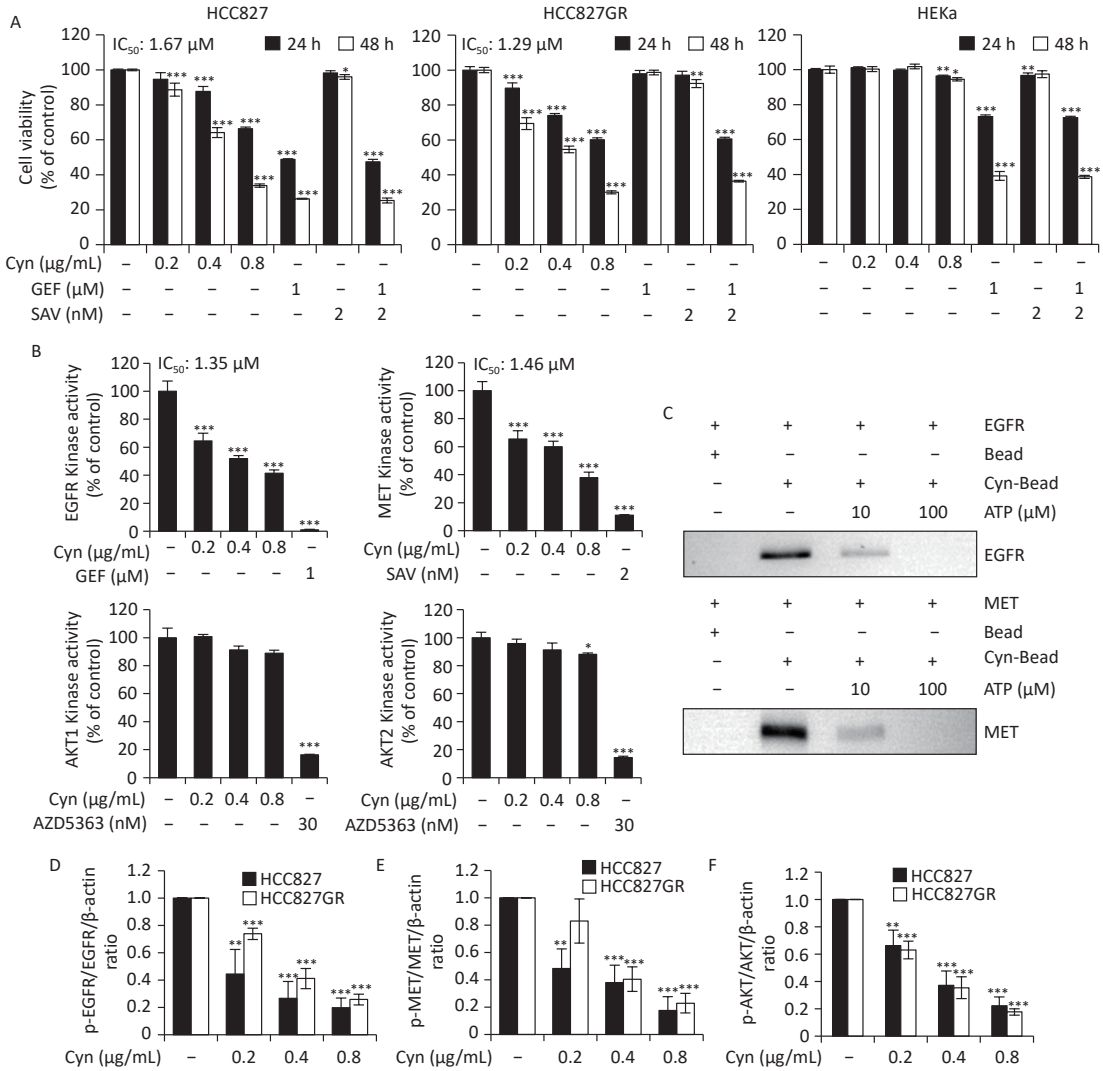

Figure 1. NSCLC cell growth inhibition and kinase inhibition induced by Cynaropicrin. (A) HCC827, HCC827GR, and HEKa cells were exposed to Cyn (0.2, 0.4, or 0.8 μg/mL), gefitinib (GEF, 1 μmol/L), or savolitinib (SAV, 2 nmol/L) for either 24 h (closed bars) or 48 h (open bars). Cell viability was assessed via the MTT assay, and IC_{50} values were determined following 48 h of incubation; for HEKa cells, additional experiments were performed to obtain the IC_{50} value. Data are reported as the mean ± standard deviation (n = 3, biological triplicate). *P < 0.05, **P < 0.01, and ***P < 0.001 versus the vehicle control. (B) The in vitro ADP-Glo kinase assay was used to measure the activities of EGFR, MET, AKT1, and AKT2 kinases. The reactions were performed with various concentrations of Cyn (0.2, 0.4, and 0.8 μg/mL) or respective inhibitors (GEF, SAV, or AZD5363) as indicated. Results are shown as the mean ± standard deviation (n = 3, biological triplicate). *P < 0.05 and ***P < 0.001 compared to vehicle control. (C) Cyn–EGFR or Cyn–MET protein interaction in vitro. Active EGFR or MET kinases (100 ng) were incubated with ATP (0, 10, and 100 μmol/L), followed by incubation with Sepharose 4B or Cyn–Sepharose 4B beads. The beads were then washed and analyzed by Western blotting to detect bound EGFR or MET proteins. Bead: Sepharose 4B; Cyn–Bead: Cyn–Sepharose 4B. (D–F) HCC827 and HCC827GR cells were treated with Cyn (0.2, 0.4, or 0.8 μg/mL) for 48 h, collected, and subjected to Western blot analysis. Graphs show densitometric analysis of p-EGFR/EGFR, p-MET/MET, and p-AKT/AKT ratios normalized against β-actin. Data are expressed as the mean ± standard deviation (n = 3, biological triplicate). **P < 0.01 and ***P < 0.001 versus vehicle control. See Supplementary Figure S2A for Western blotting. IC_{50}, half inhibitory concentration.

phosphorylation status of AKT.

Flow cytometric analysis using PI staining demonstrated a pronounced elevation in the proportion of cells in the G_2/M phase following Cyn treatment (Supplementary Figure S3). At the same time, the expression levels of cyclin B1 and cdc2 were reduced in Cyn-treated cells compared to the control cells, whereas the expression level of p27 was upregulated with Cyn treatment (Supplementary Figure 3E). These results support that Cyn induces G_2/M phase cell cycle arrest.

Next, we assessed the production of ROS in NSCLC cells exposed to Cyn by performing flow cytometry with the CellROX Green. The proportion of ROS-positive cells increased after Cyn treatment in both HCC827 and HCC827GR cells (Figure 2A). To examine whether ROS generation is critical for Cyn-induced cytotoxicity, NSCLC cells were pretreated

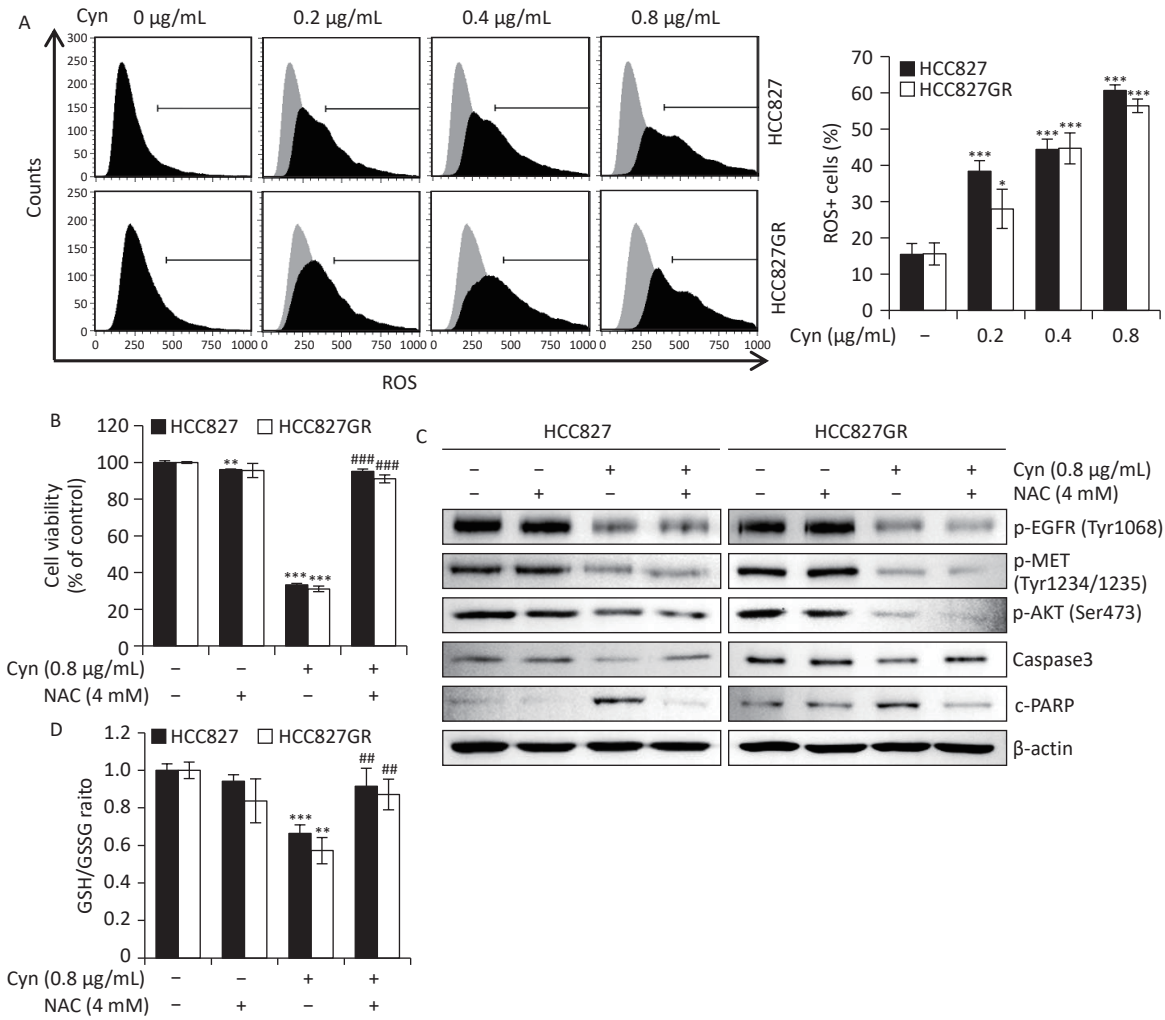

Figure 2. Induction of ROS following Cyn treatment in NSCLC cells. HCC827 and HCC827GR cells were exposed to Cyn (0.2, 0.4, or 0.8 μg/mL) for 48 h and subjected to flow cytometry with CellROX Green staining. (A) Histogram analyses of ROS production and quantification of ROS-positive cells in HCC827 (closed bars) and HCC827GR (open bars) lines. (B and C) NSCLC cells were preincubated with NAC (4 mmol/L) for 3 h, followed by treatment with Cyn (0.8 μg/mL). (B) MTT assay results for cell viability in HCC827 and HCC827GR cells following the specified treatments. (C) Western blot evaluation of p-EGFR, p-MET, p-AKT, full-length Caspase-3, and cleaved PARP (c-PARP), with β-actin serving as the loading control. (D) GSH/GSSG ratios are shown. Data are expressed as mean ± standard deviation (n = 3, technical triplicate). *P < 0.05, **P < 0.01, and ***P < 0.001 versus corresponding controls. $^{\#\#}P$ < 0.01 and $^{\#\#\#}P$ < 0.001 compared with the Cyn (0.8 μg/mL) group (Tukey's post hoc test). ROS, reactive oxygen species; Cyn, cynaropicrin; NSCLC, non-small cell lung cancer.

with N-Acetylcysteine (NAC, 4 mmol/L) for 3 h prior to Cyn exposure. The viability of cells treated with Cyn (0.8 μg/mL), measured by MTT assay, decreased to 33.3% and 31.1% in HCC827 and HCC827GR cells, respectively, but was restored to 95.2% and 91.0% following NAC pretreatment (Figure 2B). Western blotting demonstrated that the phosphorylated forms of EGFR, MET, and AKT persisted in being suppressed by Cyn regardless of NAC pretreatment. However, NAC pretreatment mitigated apoptosis-associated alterations: the reduction of caspase-3 and elevation of cleaved PARP induced by Cyn were

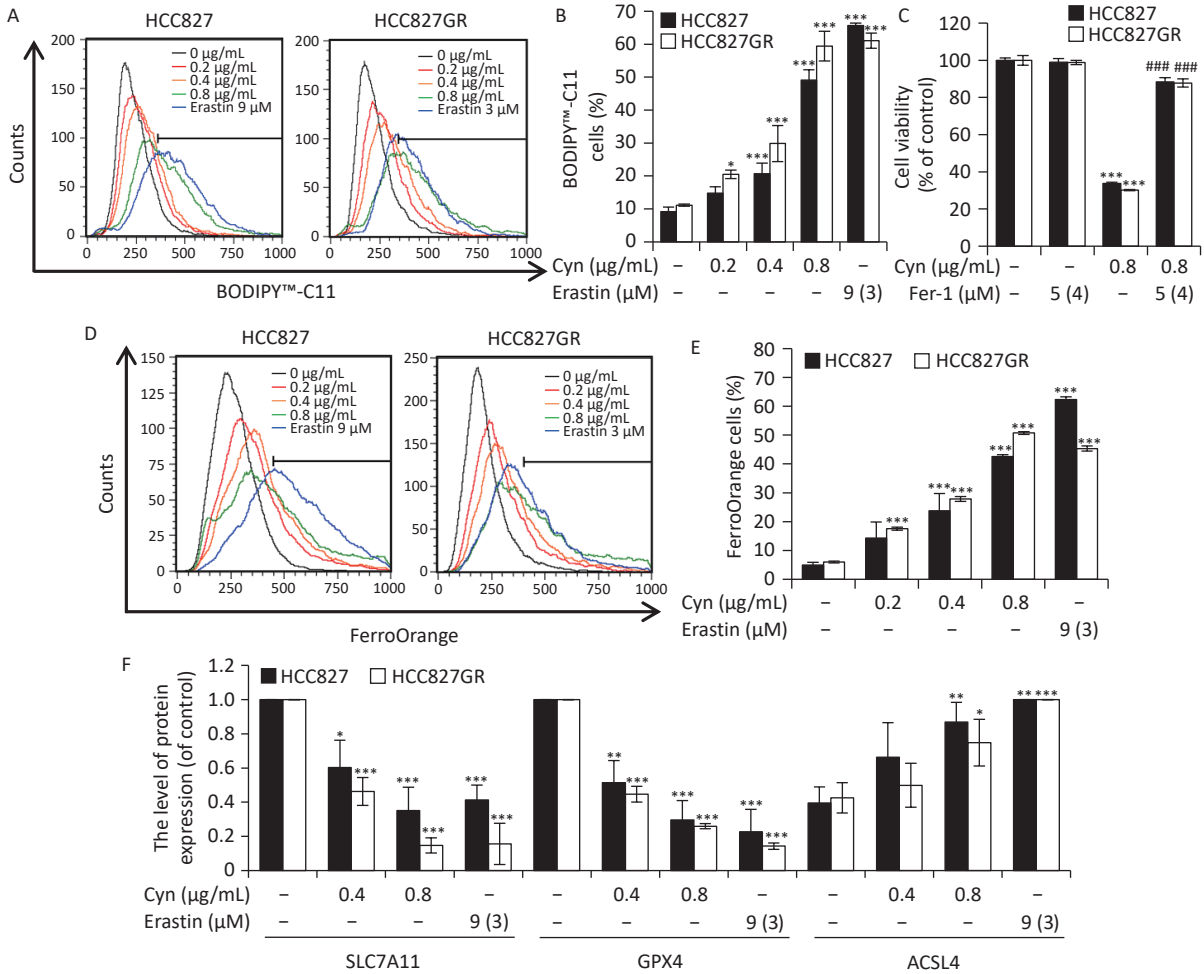

Figure 3. Ferroptosis of NSCLC cells following Cyn treatment. HCC827 and HCC827GR cells were treated with either Cyn (0.2, 0.4, or 0.8 μg/mL) or erastin (9 μmol/L for HCC827 and 3 μmol/L for HCC827GR) for 48 h and analyzed via flow cytometry with BODIPY-C11 staining or FerroOrange staining, and Western blotting analysis. (A) Lipid peroxidation, determined by BODIPY-C11 staining, is depicted in histogram format. (B) Percentage of cells displaying lipid peroxidation in HCC827 and HCC827GR cells. (C) MTT assay data evaluating cell viability in HCC827 and HCC827GR cell lines under the indicated treatments. Fer-1: ferrostatin-1 preincubation was conducted for 12 h prior to Cyn administration. Data are depicted as mean ± standard deviation (n = 3, technical triplicate). *P < 0.05, **P < 0.01, and ***P < 0.001 versus the control group. $^{\#\#\#}P$ < 0.001 compared with the Cyn (0.8 μg/mL) group (Tukey's post hoc test). (D) Histograms demonstrate FerroOrange staining. (E) Quantitative analysis of Fe^{2+}-positive cells in HCC827 (closed bars) and HCC827GR (open bars). (F) Relative expression ratios of SLC7A11, GPX4, and ACSL4 normalized to β-actin based on Western blotting analysis. See Supplementary Figure S5 for Western blotting. Data are shown as mean ± standard deviation (n = 3, biological triplicate). *P < 0.05, **P < 0.01, and ***P < 0.001 relative to the control group. Cyn, cynaropicrin; NSCLC, non-small cell lung cancer.

both reversed after NAC pretreatment (Figure 2C). The ratio of reduced glutathione (GSH) to its oxidized form (GSSG), expressed as GSH/GSSG, is an established marker for cellular antioxidant capacity (7). We determined the GSH/GSSG ratio using the GSH/GSSG-Glo Assay kit (Promega). In both HCC827 and HCC827GR cells, the relative GSH/GSSG ratio decreased to 0.66 and 0.57, respectively; however, after NAC pretreatment, this ratio increased to 0.92 and 0.87 (Figure 2D). Notably, the decrease in the phosphorylation levels of EGFR, MET, and AKT was not restored, suggesting that excessive ROS generation occurs downstream of these kinase pathways.

To evaluate whether Cyn induces apoptosis in NSCLC cells, flow cytometry was used with annexin V/PI double staining. In both HCC827 and HCC827GR cells, the proportion of cells undergoing early apoptosis (annexin V-positive and PI-negative) and late apoptosis (annexin V-positive and PI-positive) increased following Cyn exposure (Supplementary Figure S4). To assess whether Cyn promotes lipid peroxidation in NSCLC cells, flow cytometry using BODIPY 581/591 C11 staining was carried out. In HCC827 cells, lipid peroxidation levels rose from a baseline of 9.2% to 49.1% after treatment with 0.8 μg/mL Cyn. Likewise, in HCC827GR cells, this parameter increased from 11.1% to 59.4% (Figure 3A). Erastin, a recognized inducer of ferroptosis in various cancer cell types via inhibition of system x_c^- (8), elevated lipid peroxidation to 65.7% in HCC827 and 61.1% in HCC827GR cells following treatment with 3 or 9 μmol/L, respectively (Figure 3B). To examine whether Cyn-induced cytotoxicity in NSCLC cells is dependent on ferroptosis, cells were pre-incubated with Fer-1 for 12 h before Cyn treatment. Cell viability, assessed by MTT assay, declined to 33.8% and 30.2% in HCC827 and HCC827GR cells, respectively, compared to the vehicle control, but was recovered to 88.4% and 87.8% with Fer-1 pretreatment (Figure 3C). Elevated iron levels, along with lipid peroxidation, are recognized as key determinants of ferroptosis. To clarify whether the cytotoxic effect of Cyn involves ferroptosis, intracellular ferrous iron levels were measured in NSCLC cells treated with Cyn using flow cytometry and FerroOrange staining (Figure 3D). In HCC827 cells, the proportion of Fe^{2+}-positive cells increased from 5.00% in control to 14.3%, 23.8%, and 42.6% with rising Cyn concentrations; corresponding levels in HCC827GR cells increased from 6.0% to 17.6%, 27.9%, and 50.7%. Treatment with erastin also produced an increase in Fe^{2+}-positive cell ratios in NSCLC cells (Figure 3E). Furthermore, western blot analysis indicated that Cyn decreased the protein abundance of SLC7A11 and GPX4, while upregulating ACSL4 expression (Figure 3F and Supplementary Figure S5). ACSL4 selectively channels long-chain polyunsaturated fatty acids to pathways leading to lipid peroxidation-associated cell death, while SLC7A11 and GPX4 act to inhibit ferroptosis[9].

To determine whether Cyn-induced cytotoxicity involves a reduction in mitochondrial membrane potential, NSCLC cells exposed to Cyn were subjected to flow cytometry analysis with JC-1 staining. The percentage of HCC827 and HCC827GR cells displaying JC-1 green fluorescence increased following exposure to Cyn (Supplementary Figure S6A). To evaluate whether the reduction in mitochondrial membrane potential results in caspase activation, cells were additionally analyzed by flow cytometry using a multi-caspase assay kit (Supplementary Figure S6B). The proportion of NSCLC cells in the quadrant positive for both multi-caspase and 7-AAD increased after treatment with 0.8 μg/mL Cyn (Supplementary Figure S6C). Western blot analysis demonstrated that Cyn treatment reduced the expression of Bcl-2 and full-length caspase-3 and increased Bax and cleaved PARP levels (Supplementary Figure S6D). Furthermore, pretreatment with Z-VAD-FMK (12 μmol/L) for 3 h restored the viability of HCC827 and HCC827GR cells to 72.4% and 65.2%, respectively, contrasted with the reductions to 26.5% and 15.9% after Cyn treatment alone (Supplementary Figure S6E).

To evaluate whether the antiproliferative activity of Cyn extends across NSCLC cells with diverse genetic backgrounds, the IC_{50} values of Cyn were determined in additional NSCLC cell lines (Supplementary Table S1; Supplementary Figures S7A and S7B). We noticed the relatively lower IC_{50} values in EGFR-mutant NSCLC cell lines compared with other NSCLC cell lines, which may reflect their greater dependence on constitutively active EGFR signaling. Although EGFR-mutant NSCLC cells generally showed greater sensitivity to Cyn, H1299 cells, which express wild-type EGFR, also exhibited marked sensitivity. This suggests that mechanisms beyond constitutive EGFR signaling contribute to the anticancer activity of Cyn. Further investigation is warranted to identify additional molecular determinants that influence the responsiveness of NSCLC cells to Cyn. Cyn did not exhibit cytotoxicity against HEKa, a non-cancerous epidermal keratinocyte (Figure 1A), suggesting its potential

selectivity for inhibiting the growth of malignant cells. Although Cyn exhibits lower overall potency in terms of cytotoxicity and kinase inhibition compared to GEF or SAV, it showed reduced toxicity toward HEKa cells compared to GEF or SAV.

In addition, Cyn-induced apoptosis and lipid peroxidation were further observed in other NSCLC cell lines (H1650, H1975, and H1299) using Annexin V/PI double staining and BODIPY 581/591 staining (Supplementary Figures S7C–S7E). These results suggest that Cyn treatment may induce lipid peroxidation across a variety of NSCLC cells. Compared with other natural EGFR or MET inhibitors, such as 3-acetyl-O-rubiarbonol[10], Cyn exhibited comparable inhibitory potency and multitarget activity, suggesting its potential as a dual-action anticancer compound. It remains to be determined how dual targeting of EGFR and MET by Cyn differs mechanistically from that of other phytochemicals. Furthermore, whether and how the dual inhibition of EGFR and MET contributes to the ferroptotic process remains to be elucidated. Additionally, the relative contributions of the apoptotic and ferroptotic pathways to Cyn-induced cytotoxicity remain to be determined. The present study was limited by the absence of pharmacokinetic analyses, which would provide important insights into the bioavailability of Cyn. In addition, future studies should examine GPX4 expression at the mRNA level to clarify its regulatory mechanism. The current study is limited by the lack of in vivo validation. To advance the development of Cyn-based therapeutics, its bioavailability, stability, and safety must be systematically evaluated in animal models.

In summary, our findings establish that Cyn inhibits the proliferation of NSCLC HCC827 cells even in the presence of GEF resistance. Cyn treatment suppressed the kinase activities of EGFR, MET, and AKT, induced cell cycle arrest, and enhanced ROS generation, facilitating both ferroptosis and apoptosis. These results indicate that Cyn exhibits therapeutic promise for the treatment of NSCLC with GEF resistance and merits further investigation.

Funding This work was supported by the National Research Foundation of Korea (NRF) Grants funded by the Korea government (MSIT) (No. RS-2022-NR070862, No. RS-2024-00336900). The funders had no role in study design, data collection and analysis, decision to publish, or preparation of the manuscript.

Competing Interests The authors declare no competing interests.

Ethics Not applicable.

Authors' Contributions Conceptualization, Data curation, Investigation, Methodology, and Writing - original draft & review & editing: **A-Young Nam**. Data curation, Methodology, Validation, and Writing – review & editing: **Na Yeong Lee**. Resources, Validation, and Formal analysis: **Goo Yoon, Jin Woo Park**. Validation and Formal analysis: **Yung Hyun Choi, Joon-Seok Choi**. Software, Project administration, and Writing – review & editing: **Sang Hoon Joo**. Writing – review & editing, Supervision, Project administration, and Funding acquisition: **Jung-Hyun Shim**.

Acknowledgements Not applicable.

Data Sharing The supplementary materials will be available in www.besjournal.com.

[&]These authors contributed equally to this work.

[#]Correspondence should be addressed to Jung-Hyun Shim, PhD, Tel: +82-61-450-2684, E-mail: s1004jh@mokpo.ac.kr, s1004jh@gmail.com; Sang Hoon Joo, PhD, Tel: +82-53-850-3614, E-mail: sjoo@cu.ac.kr

Biographical notes of the first authors: A-Young Nam, PhD candidate, majoring in pharmaceutical biochemistry, E-mail: ayang2@mokpo.ac.kr; Na Yeong Lee, PhD candidate, majoring in pharmaceutical biochemistry, E-mail: ny9404@mokpo.ac.kr

Received:

Accepted:

REFERENCES

1. Turke AB, Zejnullahu K, Wu YL, et al. Preexistence and clonal selection of *MET* amplification in *EGFR* mutant NSCLC. Cancer Cell, 2010; 17, 77−88.
2. Engelman JA, Zejnullahu K, Mitsudomi T, et al. *MET* amplification leads to gefitinib resistance in lung cancer by activating ERBB3 signaling. Science, 2007; 316, 1039−43.
3. Jagadeeswaran R, Jagadeeswaran S, Bindokas VP, et al. Activation of HGF/c-Met pathway contributes to the reactive oxygen species generation and motility of small cell lung cancer cells. Am J Physiol Lung Cell Mol Physiol, 2007; 292, L1488−94.
4. Shimoda H, Ninomiya K, Nishida N, et al. Anti-hyperlipidemic sesquiterpenes and new sesquiterpene glycosides from the leaves of artichoke (*Cynara scolymus* L.): structure requirement and mode of action. Bioorg Med Chem Lett, 2003; 13, 223−8.
5. Seo SY, Joo SH, Lee SO, et al. Cynaropicrin induces the apoptosis of colorectal cancer cells by elevating reactive oxygen species and activating the JNK/p38 MAPK. Am J Cancer Res, 2025; 15, 2140−52.
6. Trott O, Olson AJ. AutoDock Vina: improving the speed and accuracy of docking with a new scoring function, efficient optimization, and multithreading. J Comput Chem, 2010; 31, 455−61.
7. Tobwala S, Fan WL, Hines CJ, et al. Antioxidant potential of *Sutherlandia frutescens* and its protective effects against

oxidative stress in various cell cultures. BMC Complement Altern Med, 2014; 14, 271.
8. Joo SH, Cho YY, Shim JH. Targeting ferroptosis to overcome drug resistance in cancer: molecular mechanisms and therapeutic prospects. Biomol Ther, 2026; 34, 18−29.
9. Feng L, Zhao KK, Sun LC, et al. SLC7A11 regulated by NRF2 modulates esophageal squamous cell carcinoma radiosensitivity by inhibiting ferroptosis. J Transl Med, 2021; 19, 367.
10. Nam AY, Joo SH, Lee NY, et al. 3-O-acetylrubiarbonol B preferentially targets EGFR and MET over rubiarbonol B to inhibit NSCLC cell growth. PLoS One, 2025; 20, e0329706.